Article ID: 1003－6326(2004)05－1012－05

Synthesis and electrochemical properties of nanocrystalline $Li[Li_{1/3}Ti_{5/3}O_4]$ by complex sol-gel method①

YANG Jian-wen(杨建文), ZHONG Hui(钟 晖), ZHONG Hai-yun(钟海云),
DAI Yan-yang(戴艳阳), LI Jian(李 荐), ZHAO Xuan(赵 绚)
(School of Metallurgical Science and Engineering, Central South University, Changsha 410083, China)

Abstract: $Li[Li_{1/3}Ti_{5/3}O_4]$ spinel-framework structure material is a kind of great interest for negative electrodes in energy storage cell. The synthesis of nanocrystalline $Li[Li_{1/3}Ti_{5/3}O_4]$ by sol-gel method using inorganic compounds and citric acid is developed, and single phase powder is obtained above 700 ℃. The electrochemical performances of $Li[Li_{1/3}Ti_{5/3}O_4]$ cathodes in lithium cell are studied. Special capacities are 131 $mA\cdot h\cdot g^{-1}$ at 0.5C rate and 154 $mA\cdot h\cdot g^{-1}$ at 0.1C in cycle test. No passivation layer is formed on $Li[Li_{1/3}Ti_{5/3}O_4]$ anode in lithium ion battery, and it is much safer than lithium metal and carbonaceous anodes. Faradic impedance in the charged cell is remarkably higher than that in discharged state, which is caused by distinct conductivities of $Li[Li_{1/3}Ti_{5/3}O_4]$ and $Li_2[Li_{1/3}Ti_{5/3}O_4]$.

Key words: $Li[Li_{1/3}Ti_{5/3}O_4]$; synthesis; sol-gel method; electrochemical properties
CLC number: TM 911 **Document code:** A

1 INTRODUCTION

Spinel $Li[Li_{1/3}Ti_{5/3}O_4]$ is a very attractive electrode material for its excellent cycle life and promising charging rate in rechargeable energy storage cells. During electrochemical reactions consisting of electron and lithium ion insertion into or extraction from it, its lattice constant changes very slightly, so it is considered a "zero-strain" insertion compound[1-3]. This material was successfully used as anode coupled with high potential cathode materials ($LiMn_2O_4$, $LiCoO_2$ or active carbon fiber) to provide a cell or hybrid supercapacitor with an operating voltage of 2.5 V[4-8]. The electrochemical behavior of $Li[Li_{1/3}Ti_{5/3}O_4]$ has already been studied by previous authors[9, 10]. There is a plateau at around 1.55 V vs. Li/Li^+ corresponding to the two-phase coexistence of the initial spinel and a phase of stoichiometry $Li_2[Li_{1/3}Ti_{5/3}O_4]$[3, 9]. In the spinel notation of $Li[Li_{1/3}Ti_{5/3}O_4]$, lithium ions occupy all tetrahedral 8a sites, lithium ions and titanium ions are located at octahedral 16d sites with ratio of Li: Ti= 1: 5, and oxygen ions are at 32e sites. During the interaction of Li^+ into the $Li[Li_{1/3}Ti_{5/3}O_4]$ structure, Li^+ begins to occupy 16c sites. Then Li^+ in the tetrahedral 8a sites also migrates to 16c sites. Eventually, all 16c sites are occupied by Li ions. The process of the insertion of Li^+ into $Li[Li_{1/3}Ti_{5/3}O_4]$ spinel structure was described as follows:

$$Li_{8a}[Li_{1/3}Ti_{5/3}]_{16d}O_{4\ 32e} + Li^+ + e = Li_{2\ 16c}[Li_{1/3}Ti_{5/3}]_{16d}O_{4\ 32e} \quad 1.5\ V\ vs.\ Li/Li^+ \qquad (1)$$

Each $Li[Li_{1/3}Ti_{5/3}O_4]$ can accommodate one lithium ion. The theoretic specific capacity corresponding to the Eqn. (1) is 175 $mA\cdot h\cdot g^{-1}$, and its practical specific capacity is 120－165 $mA\cdot h\cdot g^{-1}$.

Electrochemical performance of transition metal oxides depends on starting materials and preparation conditions. In most studies, $Li[Li_{1/3}Ti_{5/3}O_4]$ have been synthesized by a solid-state reaction of anatase TiO_2(ana-TiO_2) with Li_2CO_3 or $LiOH\cdot H_2O$. This process requires high temperature (800－1 100 ℃), long time and repeatedly grinding and calcinations[3, 4, 11]. These conventional methods suffer from inherent disadvantage of inhomogeneous mixing of solid constituents giving rise to local compositional variations, which can be eliminated by long-time diffusion of reactant ions or repeated calcinations and grinding. The processes may result in non-homogeneity, irregular morphology, large particle sizes, broad particle size distribution, poor control of stoichiometry, and contaminating from the grinding media affecting the ultimate properties of interest. Sol-gel is a desirable method for preparing electrode materials with good homogeneity, uniform morphology, and narrow size distribution[12]. Studies on the preparation of nanocrystalline $Li[Li_{1/3}Ti_{5/3}O_4]$ by sol-gel method are scarce. Expensive organic compounds are

① **Received date:** 2004－03－09; **Accepted date:** 2004－05－17
Correspondence: YANG Jian-wen, PhD candidate; Tel: +86-731-8830423, 13077300476; E-mail: zhy@mail.csu.edu.cn

commonly used as raw materials[13-15]. In this paper, we report the synthesis of nanocrystalline Li[$Li_{1/3}Ti_{5/3}O_4$] using the sol-gel method by inorganic compounds and nitric acid. Characteristics and electrochemical behaviors of the product are discussed.

2 EXPERIMENTAL

2.1 Synthesis of Li[$Li_{1/3}Ti_{5/3}O_4$]

Analytical reagent grade $TiCl_4$, HCl, $LiOH \cdot H_2O$, $C_3H_4(OH)(CO_2H)_3$ and $NH_3 \cdot H_2O$ were used as starting materials. $TiCl_4$ is a very volatile and excitive liquid. In order to be convenient, $TiCl_4$-HCl solution was prepared by dissolving $TiCl_4$ in 3 $mol \cdot L^{-1}$ HCl with ice water bath. Titanium content was analysed gravimetrically as TiO_2 by calcinating the $Ti(OH)_4$ precipitate.

$LiOH \cdot H_2O$ and $TiCl_4$-HCl solutions were respectively added into $C_3H_4(OH)(CO_2H)_3$ and $NH_3 \cdot H_2O$ aqueous solutions in proportion corresponding to stoichiometric $Li_{4/3}Ti_{5/3}O_4$ composition. The mixture was agitated and heated until forming thin-brown sol at 70 – 80 ℃, and then dried to form loose drying straw yellow gel at 150 ℃. White powder of spinel Li[$Li_{1/3}Ti_{5/3}O_4$] was obtained by calcinating the gel in air at 800 ℃ for 4 h. A flow chart of the synthesis procedure is shown in Fig. 1.

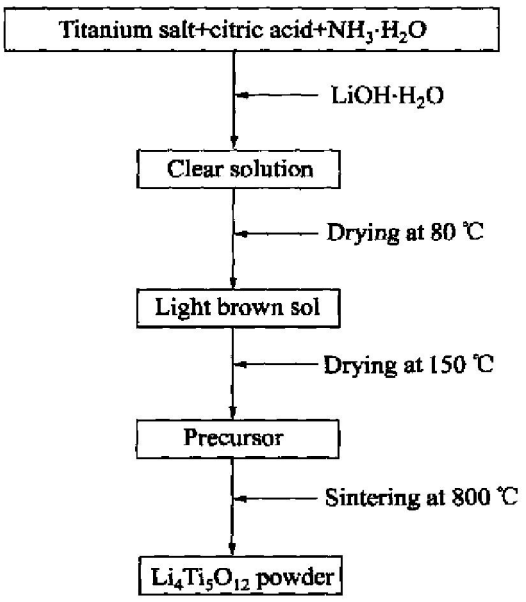

Fig. 1 Flow chart for synthesis procedure of $Li_4Ti_5O_{12}$ by sol-gel method

2.2 Characterizations

The thermogravimetric and differential thermal analysis(TGA-DTA) were performed with α-Al_2O_3 as the reference substance at a heating rate of 20 ℃ · min^{-1}, and an air flow of 100 mL · min^{-1}. The structure and morphology of the oxide powder prepared were characterized by several techniques. Powder X-ray diffraction(XRD) patterns were collected using a D/max-rA diffractometer (Japan) with Cu K_α radiation(λ= 1.540 56 Å) over the range $10° \leqslant 2\theta \leqslant 70°$. Li[$Li_{1/3}Ti_{5/3}O_4$] particle size distribution was determined by laser particle analyticlmeter (CILAS 1064 Liquid). The scanning electron microscope (JSM-5600LV) was used to observe the morphology and agglomeration.

The Li/Li[$Li_{1/3}Ti_{5/3}O_4$] coin cells were constructed for the electrochemical tests. The composite cathode was prepared by suspending 80% active material, 10% acetylene black and 10%(mass fraction) polyvinylidene difluoride(PVdF) binder in N-methyl pyrrolodone(NMP). The slurry was painted on Al foil with a doctor blade. The electrodes were dried under vacuum at 150 ℃ for 10 h before using. Lithium foil was used as anode and reference, and 1 mol/L $LiPF_6$ in ethylene carbonate (EC)/1, 2-dimethoxyethane (DME) solution (1∶1 in volume) as electrolyte. The cells were assembled in a high purity argon filled glove-box. All the electrochemical tests were carried out at room temperature. Cyclic voltammogram, charge/discharge tests and AC-impedance spectra measurement were carried out using CHI660B electrochemical work station system.

3 RESULTS AND DISCUSSION

3.1 Synthesis and characterizations

Fig. 2 shows TGA and DTA curves of the fresh precursor powder. Mass loss of 3% below 200 ℃, and that the precursor powder changes gradually yellow are due to the partially decomposition or oxidation of citric acid and evaporation of water. The second net 15% mass loss, and that the precursor gel has converted brown, show that oxidation of citric acid and decomposition of its ammonium salt correspond to an endothermic peak at 247 ℃. The third net 55% mass loss between 300 ℃ and 500 ℃ can be ascribed to complexes decomposition and the combustion of redundant carbon from the decomposition of citric acid in accordance with two strong exothermic peaks at 436 ℃ and 483 ℃ in the DTA curve. This is the evidence of thermal decomposition of titanium complex with citric acid[13]. There isn't any mass loss ranging 500 ℃ to 900 ℃ and endothermic or exothermic peak. No clear exothermic peak corresponding to Li[$Li_{1/3}Ti_{5/3}O_4$] crystallization is found; and it has been probably formed during the strong exothermic process. Such assumption has been confirmed with X-ray diffraction pattern obtained when the sample was heated at 483 ℃.

Orthogonal tests indicate that higher special capacity of Li[$Li_{1/3}Ti_{5/3}O_4$] is delivered by precursor calcined at 800 for 4h in air. According to TG-DT

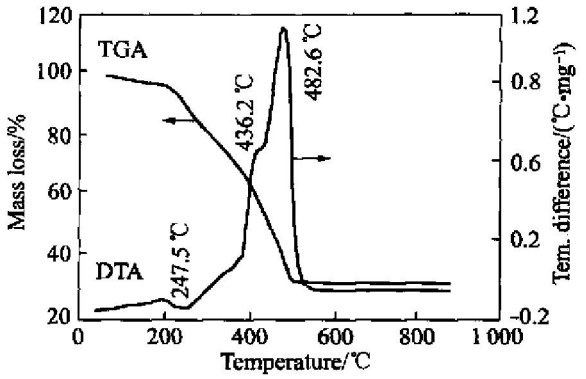

Fig. 2 TGA-DTA curves of precursor powder

analysis, X-ray diffraction measurements were carried out for the gel precursor calcined in air at different temperatures for 4 h. The XRD patterns of powders obtained are shown in Fig. 3. There are many peaks corresponding to Li [$Li_{1/3}Ti_{5/3}O_4$] (signed in Fig. 3 (800 ℃)) and Li_2TiO_3, ana-TiO_2 etc (signed in Fig. 3(483 ℃)) in the sample heated at 483 ℃, which are in accordance with the chemical transformation in the precursor powder toward Li[$Li_{1/3}Ti_{5/3}O_4$], Li-rich phase Li_2TiO_3, ana-TiO_2 and unsharpness Li_2O. Only the diffraction peaks of Li[$Li_{1/3}Ti_{5/3}O_4$] are observed (in Fig. 3(700 ℃) and (800 ℃)), and the other phases are not found in the samples after fired at above 700 ℃, which indicates that the rate of scatter of Li^+ and Ti^{4+} ions in the reaction is quickened with increasing temperature. All peaks of Li[$Li_{1/3}Ti_{5/3}O_4$] in Fig. 3(800 ℃) are sharper than those in Fig. 3(700 ℃), which shows that crystalline growth of single phase Li[$Li_{1/3}Ti_{5/3}O_4$] have occurred. The XRD pattern of the powder calcined at 800 ℃ is shown in Fig. 3(800 ℃) with a lattice parameter of a = 8.365 Å, which is in good agreement with references [1, 3, 5]. Crystallite size was calculated by using the Scherrer formula: $D = 0.9\lambda/\beta\cos\theta$, where D is the crystallite size in nm, λ is the radiation wavelength (0.154 056 nm), θ is the diffraction peak angle and β is the line width at half peak intensity. The crystallite size estimated from X-ray line broadening of the (111) peak is 36 nm.

Fig. 4 shows the scanning electron microscopy (SEM) images of the sample calcined at 800 ℃, which reflect the porous agglomerate nature of the fine powder and irregular morphology. The particle size is about 1.0 μm, which is in good agreement with laser particle size distribution analysis (in Fig. 5).

3.2 Electrochemical analysis

The cyclic voltammetric curves for a sol-gel Li[$Li_{1/3}Ti_{5/3}O_4$] electrode are shown in Fig. 6. The voltage was circularly scanned between 2.5 and 1.0 V at a scanning rate of 0.2 mV·s^{-1}. One reduction and oxidation process appears, which is in agreement with the previous reports by other methods[1, 4, 5]. It is characterized by the corresponding cathodic and anodic peak potential respectively located at 1.26 V and 1.83 V. The difference between the cathodic and anodic peak potential is about 0.6 V. It is probably caused by the different synthesis pro-

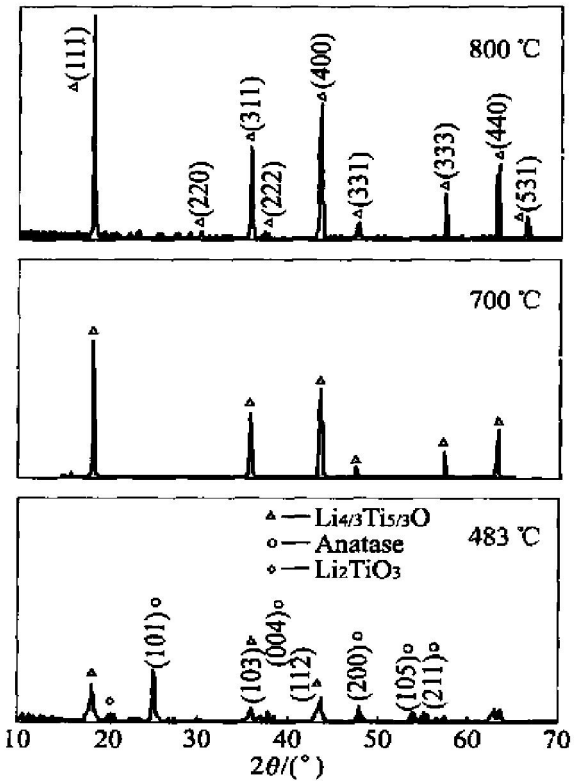

Fig. 3 XRD patterns of precursors calcined at 483 ℃, 700 ℃ and 800 ℃

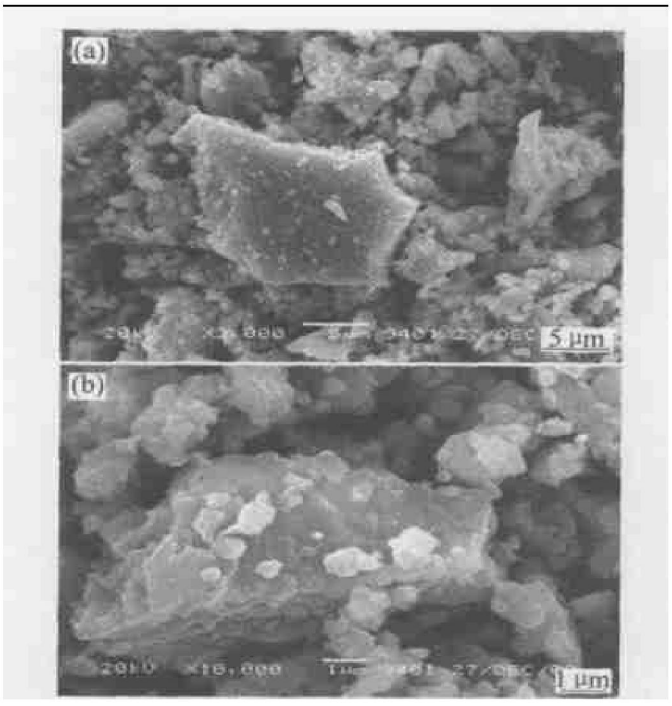

Fig. 4 SEM images of Li[$Li_{1/3}Ti_{5/3}O_4$] sample calcined at 800 ℃ for 4 h in air

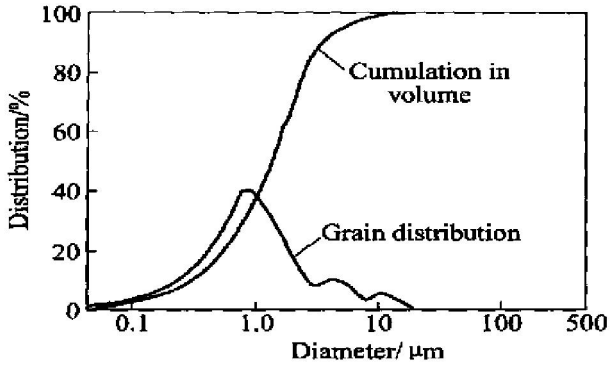

Fig. 5 Granularity analysis of $Li_4Ti_5O_{12}$

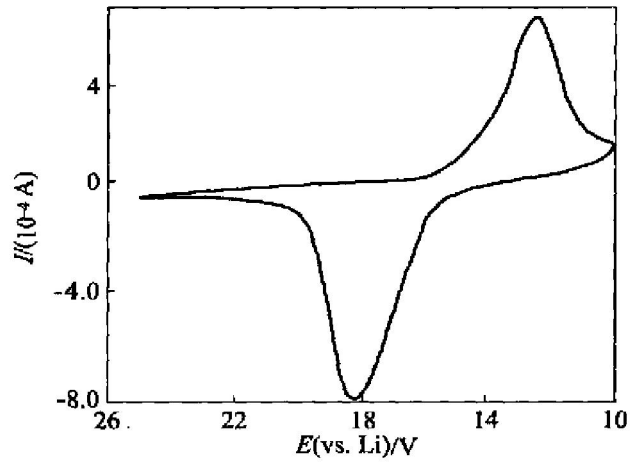

Fig. 6 Cyclic voltammogram of Li/ Li[$Li_{1/3}Ti_{5/3}O_4$] cell at scanning rate of 0.2 mV·s^{-1}

cess[5]. The reduction peak and oxidation peak current is not symmetric[4], which is possibly associated to the conductivity of titanate lithium (refer to AC impedance tests).

Fig. 7 displays the charge and discharge behavior of Li/ Li[$Li_{1/3}Ti_{5/3}O_4$] cell at constant current density at 20 ℃. The initial open-circuit voltage is 2.8 – 3.1 V. During the discharge, the voltage drops quickly down to below 2.0 V and decreases until the voltage reaches about 1.55 V, after the voltage does almost not shift corresponding to the two-phase coexistence, and 80% of above discharge capacity is in this process. When the discharged cell is charged, the voltage follows just the above process in the reverse direction. The special capacity of the first discharge is about 189 mA·h·g^{-1}. The charge-discharge curves selected from one cycle test are also shown in Fig. 7. The cell exhibits 154 mA·h·g^{-1} of rechargeable capacity at C/10 rate between 1.0 V and 3.5 V, and 131 mA·h·g^{-1} at C/2 rate between 0.8 V and 3.5 V, which does not fade rapidly upon 50 cycles.

At open-circle potential following full charge and discharge, AC impedance analysis was carried out in the frequency range of 100 kHz – 0.01 Hz with 5

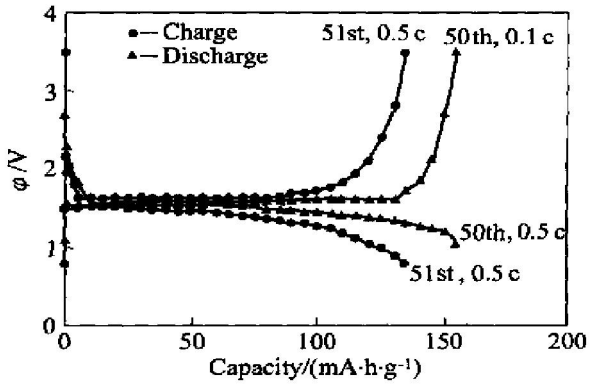

Fig. 7 Charge/ discharge cycling profiles of Li/ Li[$Li_{1/3}Ti_{5/3}O_4$] at different constant current

mV amplitude. The Nyquist plots of the cell are presented in Fig. 8. A single semicircle displays along the real axis in the high frequency rang. At middle and low frequencies, a straight line inclines to the real axis with an angle of 45°, corresponding to the Warburg impedance. Two main characteristics are observed. The first one is the absence of a second semicircle related to the presence of a passivation layer[4]. It appears that the passivation free Li[$Li_{1/3}Ti_{5/3}O_4$] anode in lithium ion battery is much safer than either lithium metal or carbonaceous anodes[5]. The second one is the higher value of the Faradic impedance at states charged in comparison with the states discharged, but their ohm impedances are the same. It is possibly due to the intrinsic electrical conductivity of lithium titanate[4], because the conductivity of Li[$Li_{1/3}Ti_{5/3}O_4$] is only 10^{-9} S·cm^{-2}; on the contrary, the conductivity of Li_2[$Li_{1/3}Ti_{5/3}O_4$] is as high as 10^{-2} S·cm^{-2}.

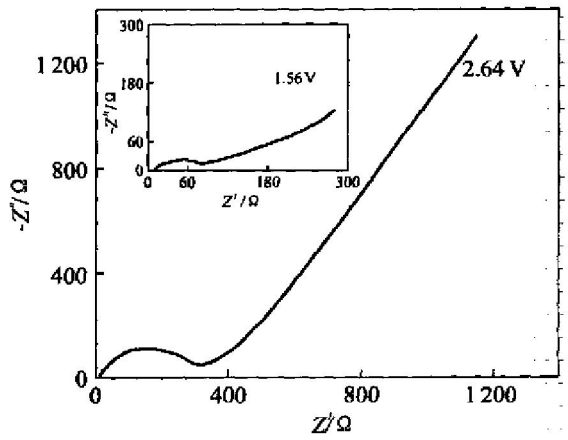

Fig. 8 AC impedance spectra of Li[$Li_{1/3}Ti_{5/3}$]O_4 cell at charge and discharge states

4 CONCLUSIONS

Single-phase spine Li[$Li_{1/3}Ti_{5/3}O_4$] was successfully synthesized from citric complexes of titanium and lithium by sol-gel method above 700 ℃ for 4 h in air. The powder prepared is irregularly porous ag-

glomerate of nanocyrstalline $Li[Li_{1/3}Ti_{5/3}O_4]$, and mean particle size is about 1.0 μm. The electrochemical properties of $Li[Li_{1/3}Ti_{5/3}O_4]$ electrodes in lithium cells were tested using voltammetric, charge-discharge and AC impedance experiments. The powder prepared at 800 ℃ for 4 h has higher specific capacity and excellent cycle-life. No passivation film formed on the surface of an anode indicates that $Li[Li_{1/3}Ti_{5/3}O_4]$ anode is much safer for battery operation than either lithium metal or carbonaceous anodes. The distinct electrical conductivities of the oxides take different effects to their electrochemical performance.

REFERENCES

[1] Ladislav K, Michael G. Facile synthesis of nanocrystalline $Li_4Ti_5O_{12}$(spinel) exhibiting fast Li insertion[J]. Electrochemical and Solid-State Letters, 2002, 5(2): A39-A42.

[2] Masatoshi M, Satoshi U, Eriko Y, et al. Development of long life lithium ion battery for power storage[J]. J Power Sources, 2001, 101: 53-59.

[3] Tstomu O, Atsushi U, Norihiro Y. Zero-strain insertion material of $Li[Li_{1/3}Ti_{5/3}]O_4$ for rechargeable lithium cells [J]. J Electrochem Soc, 1995, 142(5): 1431-1435.

[4] Paolo P P, Rita M, Lorenzo P, et al. $Li_4Ti_5O_{12}$ as anode in all-solid-state, plastic, lithium-ion batteries for low-power applications[J]. Solid State Ionics, 2001, 144: 185-192.

[5] WANG G X, Bradhurst D H, DOU S X, et al. Spinel $Li[Li_{1/3}Ti_{5/3}]O_4$ as an anode material for lithium ion batteries[J]. J Power Sources, 1999, 83: 156-161.

[6] Aurelien D P, Irene P, John G, et al. Characteristics and performance of 500F asymmetric hybrid advanced supercapacitor prototypes[J]. J Power Sources, 2003, 113: 62-71.

[7] Guerfi A, Sevigny S, Hovington P, et al. Nano-particle $Li_4Ti_5O_{12}$ spinel as electrode for electrochemical generators[J]. J Power Sources, 2003, 119-121: 87-94.

[8] Jansen A N, Kahaian A J, Kepler K D, et al. Development of a high-power lithium-ion battery[J]. J Power Sources, 1999, 81-82: 902-905.

[9] Scharner S, Weppner W, Shmid-Beumann P. Evidence of two-phase formation upon lithium insertion into the $Li_{1.33}Ti_{1.67}O_4$ spinel[J]. Journal of the Electrochemical Society, 1999, 146(3): 857-861.

[10] Jung K N, Pyun S, Kim S W. Thermodynamic approaches to lithium intercalation into $Li[Li_{1/3}Ti_{5/3}O_4]$ film electrode[J]. J Power Sources, 2003, 119-121: 637-643.

[11] Esaka T, Hayashi M, Sakaguchi H, et al. Analysis of lithium ion distribution in electrolyzed $Li_{1.33}Ti_{1.67}O_4$ by neutron computed tomography[J]. Solid State Ionics, 2002, 147: 107-114.

[12] ZHUANG Hao-ren. Thermal decomposition of PLZT citrate precursor[J]. The Chinese Journal of Inorganic Materials, 1988, 3(1): 27-31.

[13] Bach S, Pereira-Ramos J P, Baffier N. Electrochemical properties of sol-gel $Li_{4/3}Ti_{5/3}O_4$[J]. J Power Sources, 1999, 81-82: 273-276.

[14] Rho Y H, Kanamura K, Fujisaki M, el al. Preparation of $Li_4Ti_5O_{12}$ and $LiCoO_2$ thin film electrodes from precursors obtained by sol-gel method[J]. Solid State Ionics, 2002, 151: 151-157.

[15] LI Hu-lin, SHEN Cheng-min, ZHANG Xiao-gang, et al. Preparation and characterization of nanocrystalline $Li_4Ti_5O_{12}$ by sol-gel method[J]. Materials Chemistry and Physics, 2002, 78: 437-441.

(Edited by YANG Bing)